JOURNAL OF MATERIALS SCIENCE **34** (1999) 835–842

Production of Si_3N_4 by carbothermal reduction and nitridation of sepiolite

H. ARIK
Department of Metals Education, Faculty of Technical Education, Gazi University, Ankara/Turkey

S. SARITAŞ
Department of Mechanical Engineering, Faculty of Engineering and Architecture, Gazi University, Ankara/Turkey

M. GÜNDÜZ
MTA, Mineral Analysis and Technology Department, Ankara/Turkey

A study was undertaken to determine the optimum parameters for production of Si_3N_4 powders by carbothermal reduction and nitridation (CTRN) of Turkish sepiolite. Test samples were prepared by mixing 99% purity −325 mesh carbon black and −100 mesh leached brown sepiolite with C/SiO_2 molar ratios of 1.5; 3; 4; 5, and 7.5. Prepared samples were subjected to the CTRN process at temperatures of 1200, 1300, 1400 and 1450 °C for 2, 4, 8, and 16 h. The CTRN process was conducted in an atmosphere controlled tube furnace in a nitrogen flow of 4.5 cm^3/min. All products were examined by XRD and SEM-EDX to determine the transformation, morphology and chemical composition. The results showed that the best Si_3N_4 transformation occurred at 1400 °C for 16 h with C/SiO_2 molar ratio of 4.

1. Introduction

Silicon nitride (Si_3N_4) is one of the most important technical ceramics owing to its high temperature strength, toughness, wear resistance and thermal stability due to the low coefficient of thermal expansion. Because of these properties silicon nitride is a most promising material, especially for high temperature engineering applications [1–3]. A variety of methods and techniques have been employed by various investigators to produce silicon nitride powders from raw materials as silicon source [4–8] (Table I). The well-known techniques are direct reaction between silicon (Si) and nitrogen (N_2), and carbothermal reduction of silica (SiO_2) with a source of carbon and at the same time, nitridation of it with nitrogen gas [9–11]. Sepiolite, which is a hydrous magnesium silicate with the ideal structural formula $Mg_8Si_{12}O_{30}$ $(OH)_4$ $(OH_2)_4$ $8H_2O$ for the half-unit cell, was used as the source of silica for nitridation [12, 13]. Sepiolite occurs as sedimentary-type depositions in the form of pure sepolite or associated with clays or other minerals (especially dolomite). It has an orthorhombic crystal structure and occurs as fibrous form α-sepiolite and compact form β-sepiolite. Sepiolite has an outer surface area of ≤ 300 m^2/g and an internal surface area attributed to channels and micropores of ≤ 400 m^2/g. Therefore, to some extent it has a large specific surface area of 550–700 m^2/g. According to chemical composition and color, three-types of sepiolite are distinguished in the Turkish deposits, designated as white, beige and brown. The tests were carried out on the brown sepiolite having the highest grade [14, 15, 16, 17].

2. Experimental

2.1. Material

The brown sepiolite, used throughout the investigation as a source of silica, was obtained from the Türktaciri area of Turkey, which is west of Ankara. As-received samples of brown sepiolite were analysed by XRD, which indicated that the samples contain 90% sepiolite and 10% dolomite [16]. Then it was enriched by treating in HCl solution (≤ 0.1 M HCl) for removal of dolomite. During leaching, control of acid concentration (thus pH) is very important and should be maintained at pH ≤ 4. Otherwise, fibrous structure is harmed. Chemical composition of as-received and leached brown sepiolite are given in Table II.

XRD, DTA and SEM-EDX analyses were performed on the enriched brown sepiolite to investigate the effects of the enrichment process on chemical composition and fibrous morphology of the sepiolite. XRD analysis indicated that the peaks attributed to dolomite on the XRD pattern of the as-received sample had disappeared and it gave only the peaks of sepiolite (Fig. 1). DTA-TG curves showed two endothermic peaks at 101.1 °C and 333.1 °C which are related to the release of surface water and the zeolitic water, respectively, and an exothermic peak at 801.5 °C corresponding to the phase transformation which occurred in the structure of

TABLE I Various processes for synthesis of silicon nitride [8]

Process	General reaction
Nitridation of metallic silicon powder	$3\,Si + 2\,N_2 \xrightarrow{1200-1500\,^\circ C} Si_3N_4$
Carbo-thermal reduction of SiO_2 in nitrogen atmosphere	$3\,SiO_2 + 6\,C + 2\,N_2 \xrightarrow{1200-1700\,^\circ C} Si_3N_4 + 6\,CO$
Combustion synthesis	$3\,Si + 2\,N_2 \xrightarrow{700\,atm} Si_3N_4$
Vapor-phase reaction	$3\,SiCl_4 + 4\,NH_3 \xrightarrow{1100-1350\,^\circ C} Si_3N_4 + 12\,HCl$
Imide decomposition	$SiCl_4 + 6\,NH_3 \xrightarrow{-30\,to\,+70\,^\circ C} Si(NH)_2 + 4\,NH_4Cl$
	$3\,Si(NH)_2 \xrightarrow{1600\,^\circ C} Si_3N_4 + 2\,NH_3$
Laser synthesis	$3\,SiH_4 + 4\,NH_3 \xrightarrow{CO_2\,Laser} Si_3N_4 + 12\,H_2$
Plasma synthesis	$3\,Si_3H_4 + 4\,NH_3 \xrightarrow{Plasma} Si_3N_4 + 12\,H_2$
	$3\,SiCl + 4\,NH_3 \xrightarrow{Plasma} Si_3N_4 + 12\,HCl$

TABLE II Chemical analysis of as-received brown sepiolite and leached brown sepiolite (wt %)

	As-received	Leached
SiO_2	50.05	55.90
Al_2O_3	1.17	1.19
CaO	6.00	1.73
MgO	25.5	24.00
Fe_2O_3	0.49	0.66
TiO_2	0.12	0.25
Na_2O	0.05	0.04
K_2O	0.17	0.39
LOI	16.86	15.52

sepiolite (Fig. 2). SEM micrography showed that the fibrous morphology of as-received brown sepiolite was not significantly affected by the enrichment process, although the sepiolite became partly agglomerated (Fig. 3). Carbon black with 99% purity was used as the source of carbon, and its specifications are given in Table III.

TABLE III Specifications of carbon black

Reflection (%, with toluen)	325 Mesh-sieve oversize (%)	Moisture (%)	Density (g/l)	Sulfur (%)
Min. 80	Min. —	Min. —	Min. 320	Min. —
Max. —	Max. 0.1	Max. 2.5	Max. 380	Max. 1

2.2. Effect of heating on the behavior of sepiolite

Samples of the leached brown sepiolite were heated for 2 hours in a furnace open to atmosphere at temperatures of 200, 370, 800, 850 °C in relation to the temperatures

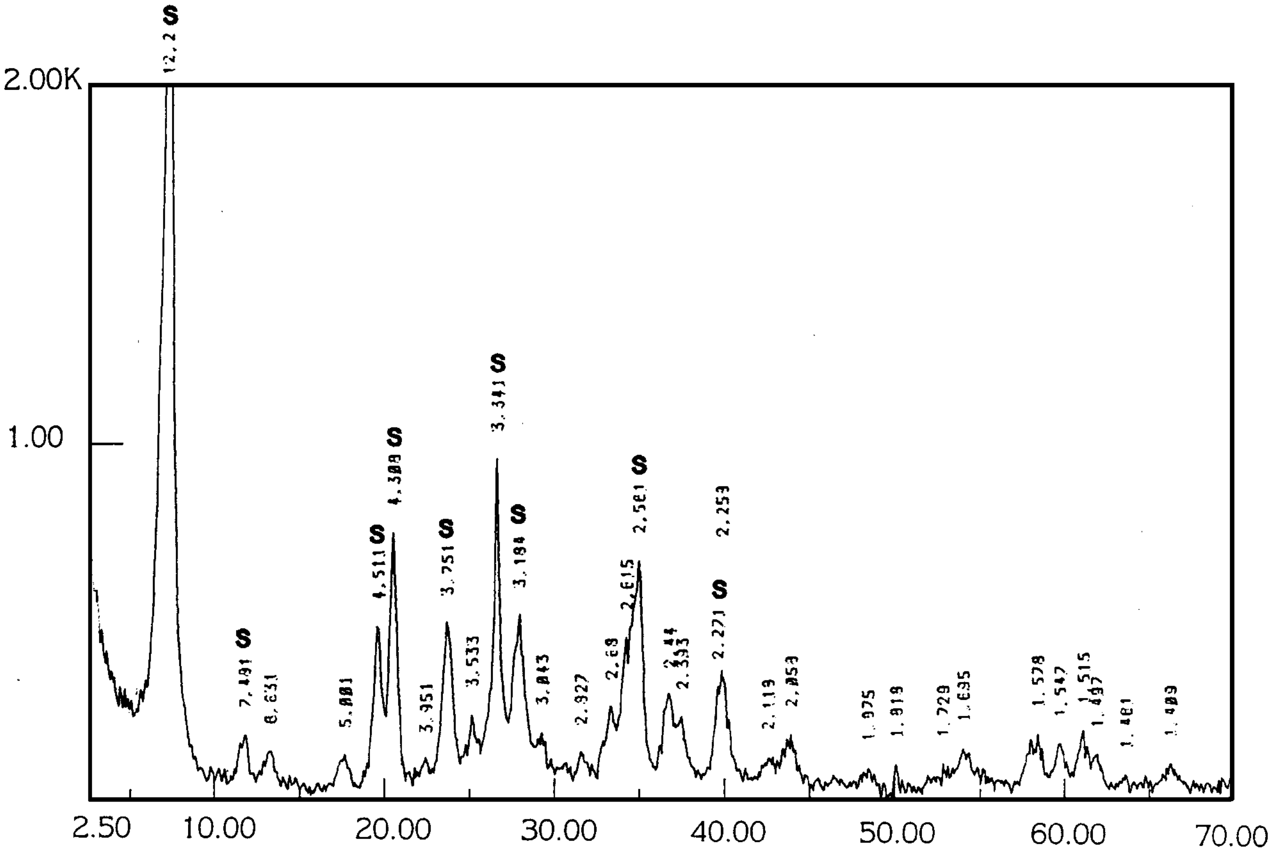

Figure 1 XRD pattern of leached brown sepiolite, (S); sepiolite.

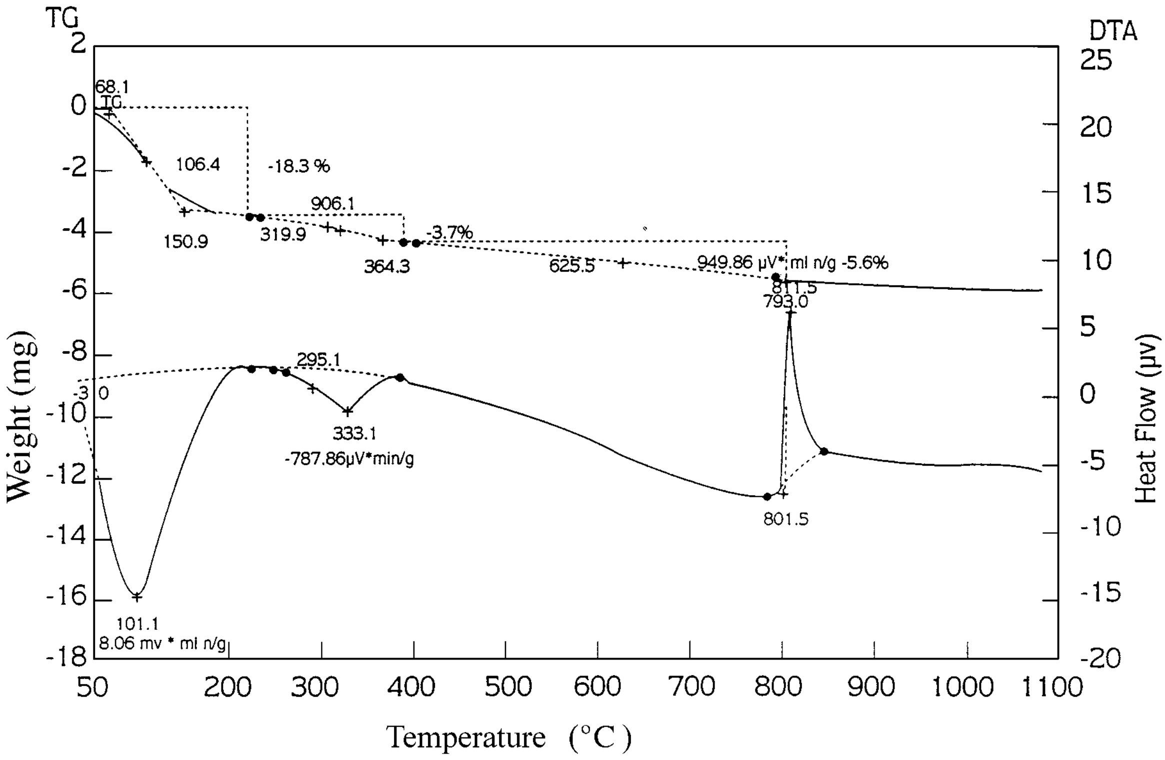

Figure 2 DTA-TG curves of leached brown sepiolite.

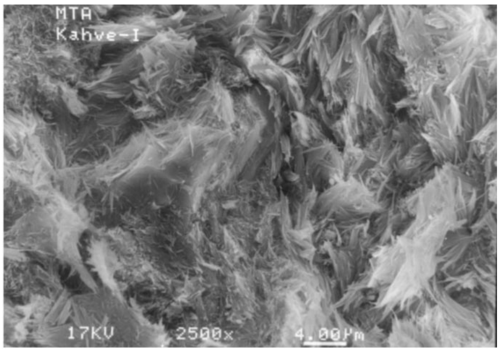

Figure 3 SEM micrograph of leached brown sepiolite.

of endothermic and exothermic peaks on the DTA-TG curves, and 1200, 1300, 1400, and 1450 °C being the temperatures chosen for the CTRN process. The products were analysed by XRD and SEM-EDX to determine the structural transformations taking place during the heating.

2.2.1. XRD and SEM-EDX analysis

XRD and SEM analysis of the products heated up to 800 °C showed no formation of phases other than those belonging to sepiolite, although the peak intensities of sepiolite was slightly decreased in relation to the temperature increase. The products maintained the fibrous morphology of sepiolite. At 800 °C, peaks of sepiolite totally disappeared while the peaks of enstatite ($MgSiO_3$) appeared (Fig. 4). The product still maintained the structure of sepiolite (Fig. 5). At 1200 °C the intensity of enstatite peaks increased relative to the peak intensities at 800 °C, and the peaks of cristobalite (SiO_2) and tridymite (SiO_2) were detected (Fig. 6). Oxides of Al_2O_3, CaO, Fe_2O_3, TiO_2, Na_2O and K_2O in the sepiolite-structure formed liquid phase due to eutectic reactions at 1200 °C, and the fibrous morphology of sepiolite agglomerated as thicker fibers (Fig. 7). At 1400 °C, cristobalite, tridymite and enstatite phases were maintained with some increase in peak intensities corresponding to more crystallization. A SEM micrograph of the product heated at 1400 °C showed the formations of uniform grains (Fig. 8).

2.3. Carbo-thermal reduction and nitridation (CTRN) of sepiolite

Sepiolite was thoroughly mixed with carbon black in C/SiO_2 molar ratios of 1.5, 3, 4, 5, and 7.5. Mixing was performed in a mill with alumina balls for 5 hours. Four gram samples of the mixtures were placed in graphite boats having dimensions 20 mm × 35 mm × 45 mm. Then the boats were placed in an atmosphere-controlled tube furnace (Fig. 9) heated to test temperature in nitrogen (N_2) flow of 4.5 cm^3/minute, and maintained for predetermined times. Under the identical test conditions, the CTRN process for 5 mixtures in various C/SiO_2 molar ratios was performed at 1200, 1300, 1400, and 1450 °C for 2, 4, 8, and 16 hours.

2.3.1. XRD and SEM-EDX analysis

All products obtained at different temperatures and times by the CTRN process were analyzed using a Rigaku-Geigerflex type XRD instrument. SEM-EDX analysis was also conducted on the products. From the XRD results it was seen that carbothermal reduction and nitridation did not take place at 1200 °C. XRD and SEM-EDX analysis results were similar to those for

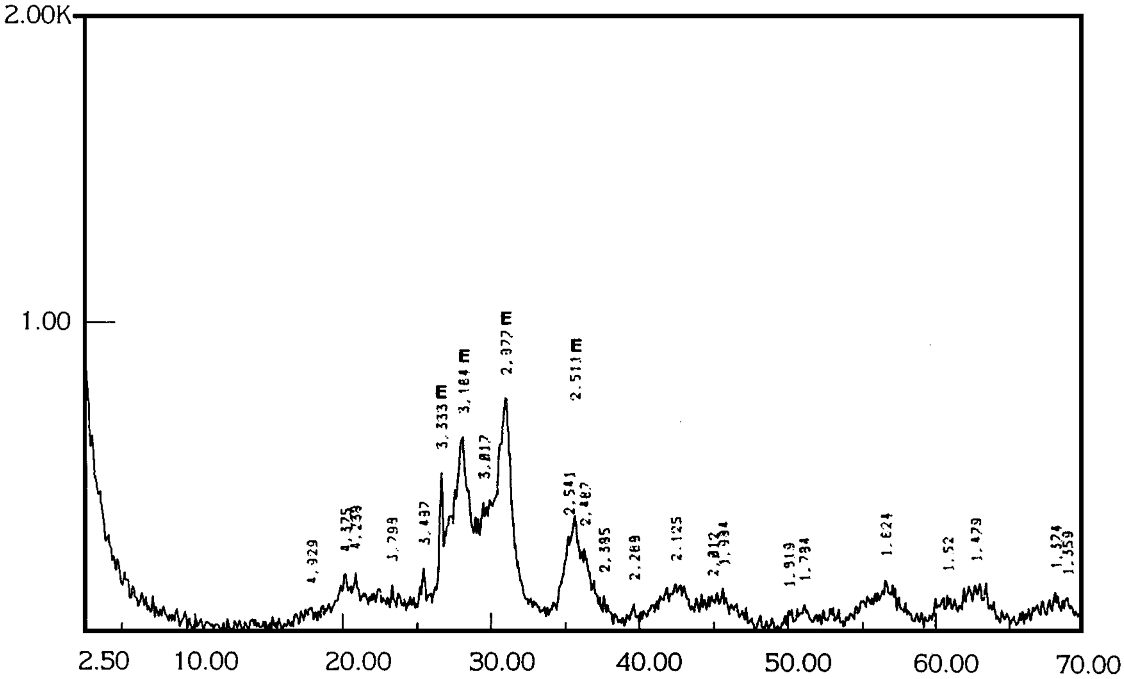

Figure 4 XRD pattern of sepiolite heated for 2 h at 800 °C, (E); enstatite.

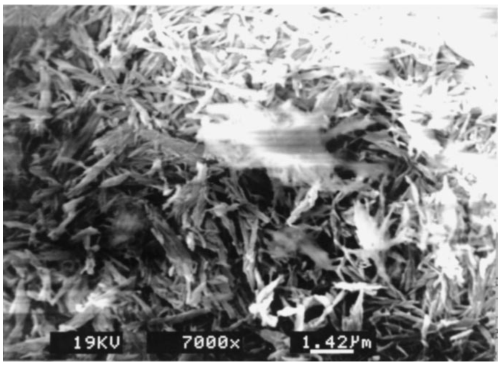

Figure 5 SEM micrograph of sepiolite heated for 2 h at 800 °C.

the fired sepiolite at the same temperature (Fig. 10). At 1300 °C, some differences were noticed on the XRD patterns suggesting some reactions taking place. XRD patterns for the products of mixtures with C/SiO_2 ratios of 1.5, 3, 4, and 5 showed the peaks of enstatite at $d = 4.037$; 3.7, fosterite at $d = 2.99$; 1.96 and Si_3N_4 at $d = 3.29$; 2.9; 1.49.

Analysis results for 2 h and 4 h treatments showed partial transformation to Si_3N_4, although most of the product was enstatite or fosterite (Fig. 11). Partial transformation to Si_3N_4 possibly resulted from reduction and nitridation of cristobalite and tridymite at 1300 °C. SEM-EDX analysis showed that the chemical

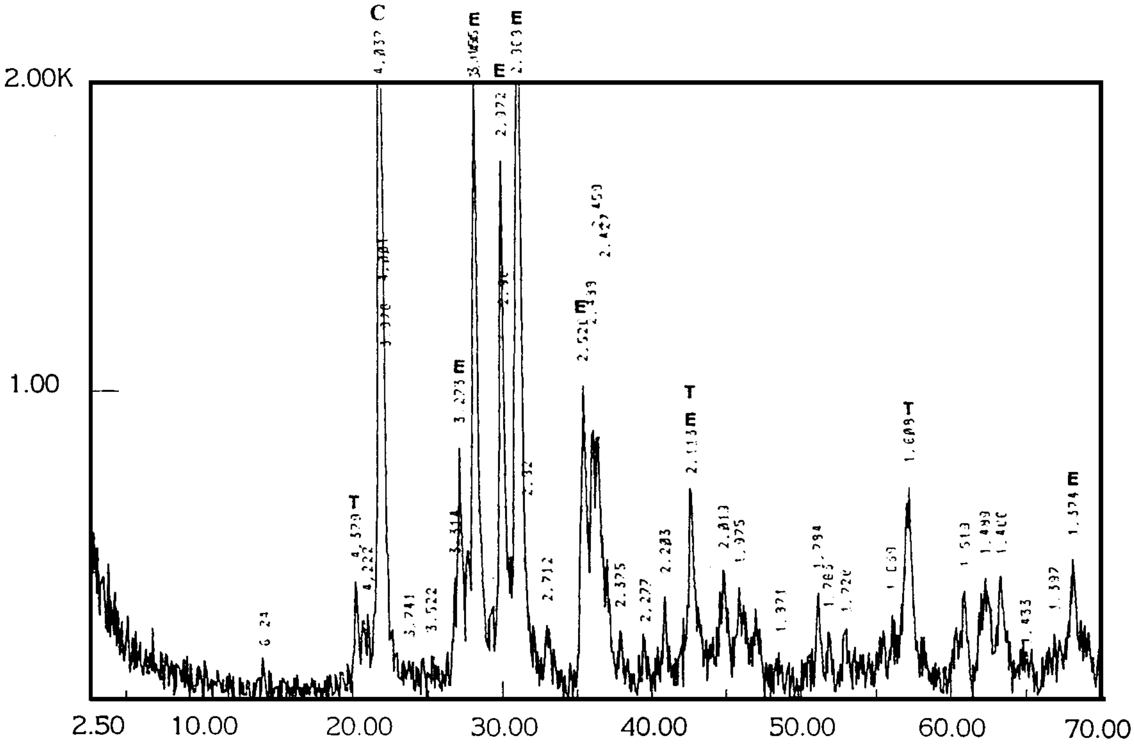

Figure 6 XRD pattern of sepiolite heated for 2 h at 1200 °C, (E); enstatite, (T); tridimide, (C); cristobalite.

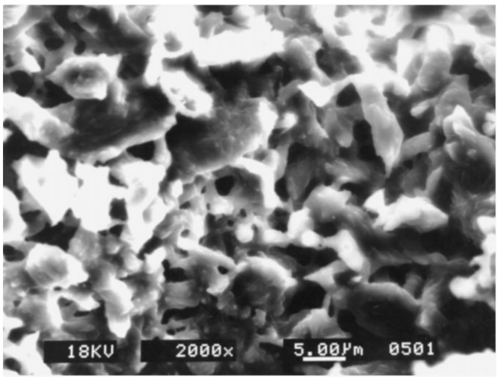

Figure 7 SEM micrograph of sepiolite heated for 2 h at 1200 °C.

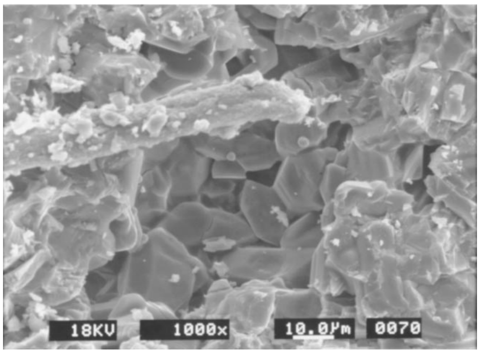

Figure 8 SEM micrograph of sepiolite heated for 2 h at 1400 °C.

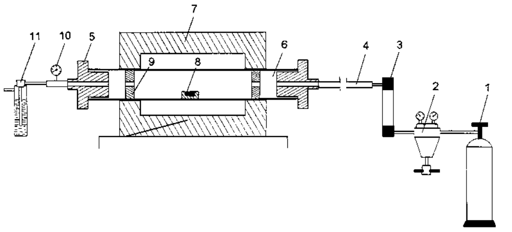

Figure 9 Carbo-thermal reduction and nitridation set-up. 1 = nitrogen cylinder, 2 = pressure regulator, 3 = rotameter, 4 = plastic hose, 5 = graphite end connector, 6 = alumina furnace tube, 7 = furnace, 8 = sample boats, 9 = anti-radiation block, 10 = manometer, 11 = dissociation bottle.

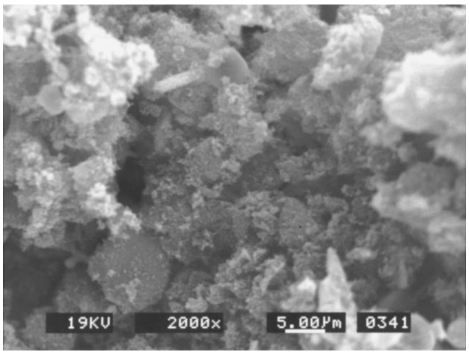

Figure 10 SEM micrograph of carbo-thermal reduction and nitridation product for C/SiO_2 molar ratio of 3 at 1200 °C.

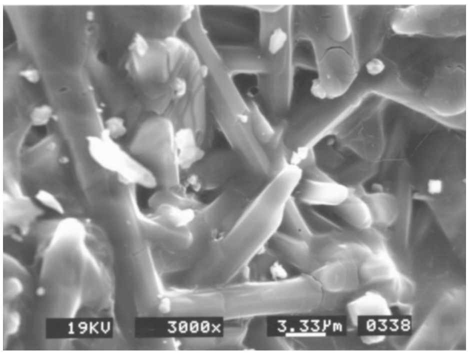

Figure 11 SEM micrograph of CTRN product for C/SiO_2 ratio of 3 at 1300 °C.

composition of sepiolite was essentially maintained. For samples with a C/SiO_2 molar ratio of 7.5, especially at 8 h and 16 h, the products had almost no enstatite and fosterite, and for the first time, peaks of $SiON_2$, $d = 3.39$ and $MgSiN_2$, $d = 2.79$ existed together with peaks of Si_3N_4. Also, peaks of Si_3N_4 $d = 1.75$ and 2.27 appeared together with the peaks previously seen. All these results indicated that reduction and nitridation reactions were not completed at 1300 °C for even 16 h treatment times.

At 1400 °C, for samples of molar ratio 1.5, enstatite and fosterite peaks were decreased but still existed even for 8 h and 16 h treatments, which showed that carbon content was not enough for complete transformation. For higher molar ratios, XRD peaks were only related to Si_3N_4 for all treatment durations, but peak intensities continuously increased as treatment time increased towards 16 hours. SEM and XRD results for molar ratio of 4 and treatment time of 2 h are shown in Fig. 12a and b. Hexagonal Si_3N_4 fibers have 0.5–3 μm width and 10–30 μm length. 16 h treatment morphology and related XRD peaks are given in Fig. 13a and b for the same molar ratio. As seen from the micrograph, globular agglomerates are composed of short hexagonal Si_3N_4 particles. The α/β ratio was about 20/80 for the 2 h treatment, but this ratio further decreased to 10/90 for the 16 h treatment. For all CTRN treatment durations there were wool-like structure formations around the corners of the boat. This was analysed as pure α-Si_3N_4 and the length of fibers were more than few millimeters. At 1450 °C, similar results were obtained for all molar ratios and treatment times but the XRD peaks were weaker. This is explained by the presence of liquid phase which will decrease reactions due to reduction in surface area.

3. Discussion

3.1. Temperature

The products of CTRN process at 1200 °C showed the same XRD peaks as the ones of fired pure sepiolite at 1200 °C which means that no reaction of SiO_2 took place. It is common believe that SiO_2 will not be reduced at this temperature [10, 18]. First Si_3N_4 peaks were recorded in CTRN processing at 1300 °C. These peaks were partly belonging to oxy-nitride peaks. Temperature is still not sufficient for complete reduction of SiO_2 [10, 18, 19] so partial reduction and nitridation took place. Transformation products are $SiON_2$ and $MgSiN_2$ which is the sign of partial reduction of MgO as well.

Major reduction of SiO_2 and MgO took place at 1400 °C. Reduced silicon was nitrided by reacting with

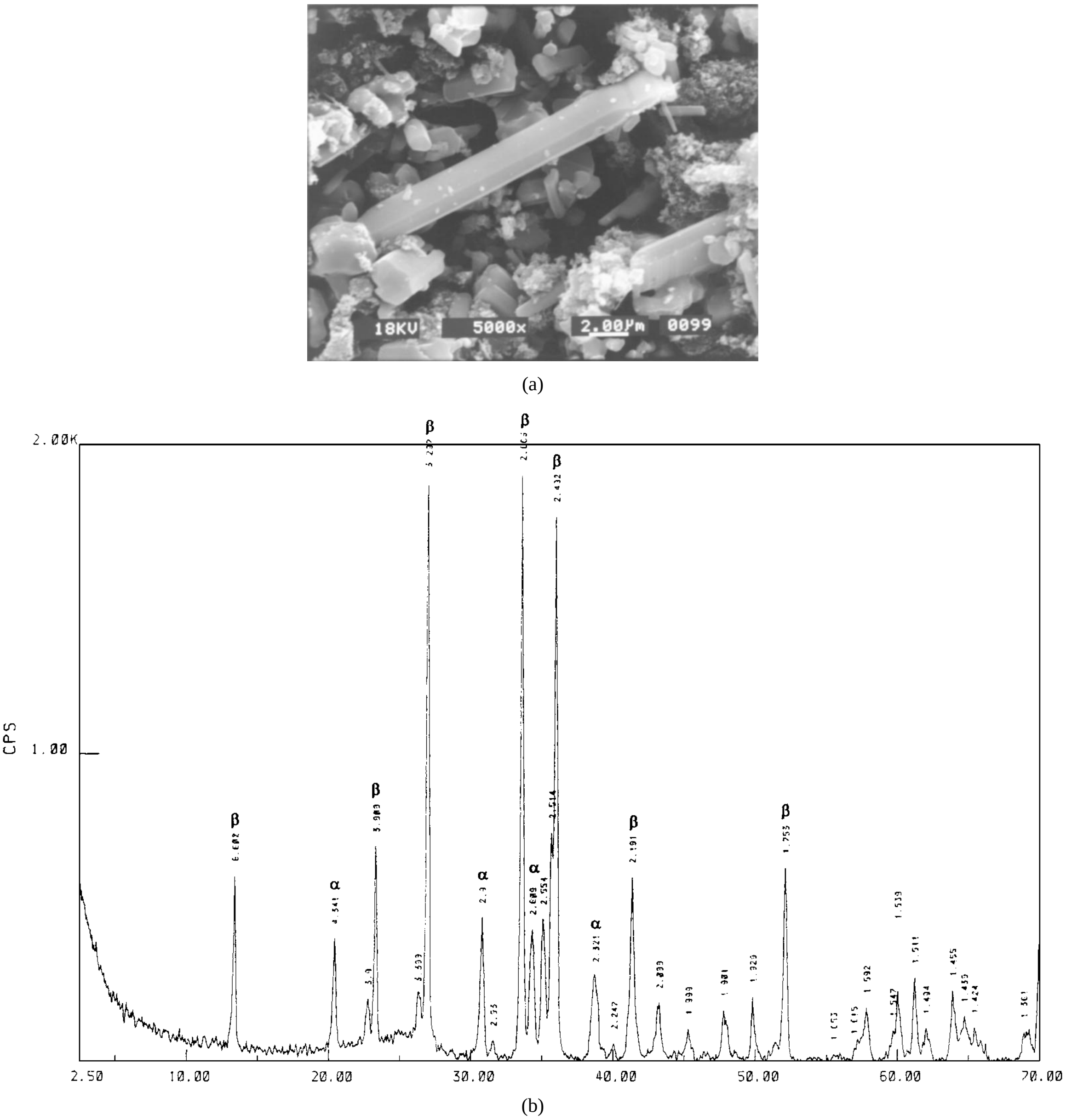

Figure 12 Fibrous Si_3N_4 of CTRN process with C/SiO_2 molar ratio of 4 at 1400 °C for 2 h. (a) SEM micrograph, (b) XRD pattern, (β); β-Si_3N_4, (α); α-Si_3N_4.

nitrogen gas, but magnesium evaporated and then carried outside the furnace by the control gas. The transformation products showed very strong Si_3N_4 peaks for all CTRN process times. Increasing CTRN temperature to 1450 °C did not produced any further increase in reduction and nitridation. This is explained by partial melting of sepiolite at this temperature. Thus microporous structure harmed and surface area dramatically reduced with the presence of liquid phase which will decrease the transport of reaction gases. 1450 °C is accepted as critical temperature in the literature for CTRN process [10]. At this temperature SiC may form instead of Si_3N_4.

3.2. Duration

The strongest Si_3N_4 peaks are seen with to 16 h CTRN processing, but at 1400 °C major Si_3N_4 formation took place for 2 h processing. In processing for this duration, a cotton-like product was observed around the graphite boats and furnace walls. These fibers are analysed as α-Si_3N_4 and explained by the following reaction:

$$SiO_{2(s)} + C_{(s)} \xrightarrow{1300-1400\,^{\circ}C} SiO_{(g)} + (CO)_{(g)}$$

$$3\,SiO_{(g)} + 3\,CO_{(g)} + 2\,N_{2(g)}$$

$$\xrightarrow{1300-1400\,^{\circ}C} \alpha\text{-}Si_3N_{4(s)} + 3\,CO_{2(g)}$$

For longer CTRN durations these cotton-like products disappeared. It is believed that α-Si_3N_4 transformed into more stable β-Si_3N_4 and then the major transformation took place in the boat direct to β-Si_3N_4 by the following reaction:

$$3\,Si + 2\,N_2 \xrightarrow{1400\,^{\circ}C} \beta\text{-}Si_3N_4$$

In the literature [19, 20, 21], higher temperatures but shorter durations are proposed for CTRN processing.

Times up to 20 hours have been reported, but 6 to 8 hours are recommended. In this work, due to micro-porous structure of the sepiolite, major Si_3N_4 formation took place at 1400 °C for 2 h treatment. Further durations should not be used since they result in β-Si_3N_4 which is not easily sintered.

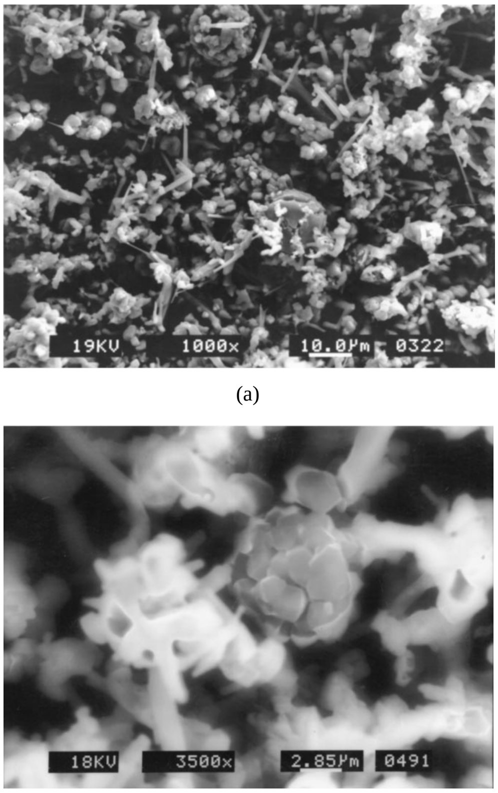

(a)

(b)

Figure 13 SEM micrograph of CTRN products for C/SiO_2 molar ratio of 4 at 1400 °C for 16 h. (a) General appearance of the transformation products. (b) High magnification micrograph showing globular transformation.

3.3. C/SiO_2 molar ratio

A C/SiO_2 molar ratio of 1.5 is not sufficient for reduction of sepiolite at all temperatures. All carbon had been consumed even for a C/SiO_2 molar ratio of 3. For a molar ratio of 4, some carbon remained as unreacted at temperatures lower than 1400 °C or times shorter than 8 hours. The literature recommends a molar ratio of 4 to 6 [10, 18, 19, 22] which is in good agreement with the present work. If there is extra carbon at the end of CTRN processing, the remaining carbon is burnt by treating the product in a furnace open to air at 650–850 °C.

3.4. Products

The XRD pattern of the sample in which maximum transformation was observed showed that all peaks were related to β-Si_3N_4. Under normal conditions, α-Si_3N_4 was produced by the CTRN process, but liquid phases of oxides such as K_2O, TiO_2, Fe_2O_3, and CaO contained in the sepiolite occurred due to eutectic reaction, leading to the formation of β-Si_3N_4 instead of α-Si_3N_4 [9, 22]. The intensity of peaks of α-Si_3N_4 on the XRD pattern of 2 h-processed product gradually decreased with the increase in duration; these peaks completely disappeared for the 16 h-processed product. As a result, formation of β-Si_3N_4 instead of α-Si_3N_4 was controlled by oxides in sepiolite and by the duration. SEM studies indicated that the powder sample contained particles of two different morphologies. Approximately 15% of the powder sample had fibrous structure of 0.5–3 μm in diameter and 10–30 μm in length, and the remainder consisted of hexagonal prisms with dimensions of 1–3 μm.

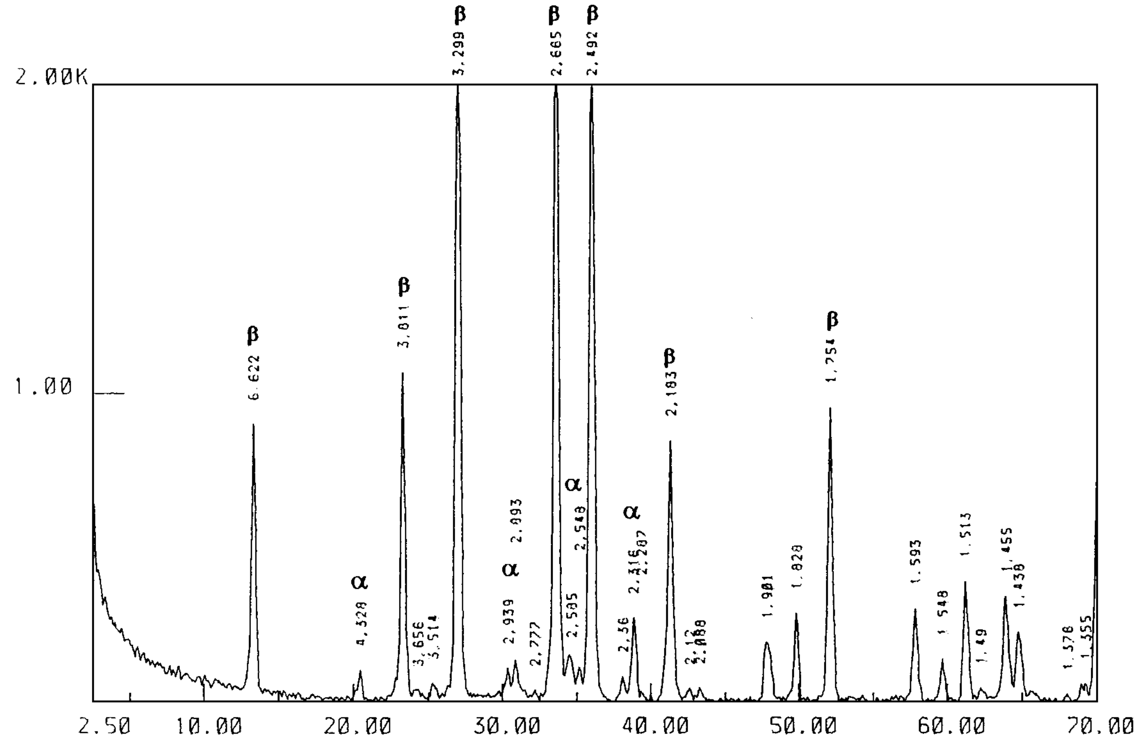

Figure 14 XRD pattern of CTRN product for C/SiO_2 molar ratio of 4 at 1400 °C for 16 h, (β); β-Si_3N_4, (α); α-Si_3N_4.

4. Conclusion

1. Si_3N_4 could be synthesized by the CTRN process from sepiolite. C/SiO_2 molar ratio of 4, temperature of 1400 °C and duration of 2 h are recommended.

2. Impurity oxides like K_2O, TiO_2, Fe_2O_3 and CaO promote formation of β-Si_3N_4 instead of the preferred α-Si_3N_4. Further cleaning of sepiolite before CTRN is necessary for removing these oxides.

3. In the CTRN process, carbon reduces SiO_2 to pure silicon. Then the pure silicon reacts with N_2 to form Si_3N_4, reacts with MgO and gets the oxygen from it, and produces SiO_2 back. These reactions continue in chain until all MgO is reduced to pure magnesium. Since the temperature is very high, the pure magnesium evaporates and is transported away by the furnace gases. The magnesium may be condensed outside the furnace and thus both Si_3N_4 and pure magnesium may be produced simultaneously from sepiolite.

References

1. G. ZIEGLER, J. HEINRICH and G. WÖTTING, *J. Mater. Sci.* **22** (1987) 3041.
2. M. HERRMANN, C. BOBERSKI, G. MICHAEL, G. PUTZKY and W. HERMEL, *J. Mater. Sci. Let.* **12** (1993) 1641.
3. K. H. JACK, *J. Mater. Sci.* **11** (1976) 1135.
4. Z. HRABE, S. KOMARNENI, P. MALLA, V. SRIKANTH and R. ROY, *J. Mater. Sci.* **27** (1992) 4614.
5. S. UMEBAYASHI and K. KOBAYASHI, *J. Amer. Ceram. Soc.* **58** (1975) 9.
6. H. MOSTAGHACI, Q. FAN, F. L. RILEY, Y. BIGAY and J. P. TORRE, *J. Brit. Ceram. Soc. Trans.* **85** (1986) 12.
7. B. KUMAR and M. M. GODKHINDI, *J. Mater. Sci. Let.* **15** (1996) 403.
8. B. W. JONG, G. J. SLAVENS and D. E. TRAUNT, *J. Mater. Sci.* **27** (1992) 6086.
9. S. A. SIDDIQI, I. HIGGINS and A. HENDRY, "*Non-oxide technical and Engineering Ceramics*" (edited by Hampshire, London and New York, 1986) pp. 119–1331.
10. S. C. ZHANG and W. R. CANNON, *J. Amer. Ceram. Soc.* **67** (1984) 691.
11. D. L. SEGAL, *J. Brit. Ceram. Soc. Trans.* **85** (1986) 184.
12. T. KIYOHIRO and R. OTSUKA, *Thermochimica Acta*, **147** (1989) 127.
13. K. INUKAI, S. TOMURA, R. MIYAWAKI, K. SHIMOSAKA, T. IRKEEÇ and N. FUJII, Proceedings of the International Geological Congress, Nagoya, Japan (1992) 115–121.
14. H. ARIK, S. KADİR, A. KÜÇÜK and S. SARITAŞ, Proceedings of the 7th National Clay Symposium, Ankara, Turkey (1995).
15. S. SARITAŞ, I. KAYABALI, M. GÜNDÜZ and B. ERDOĞAN, Proceedings of the 4th Int. Engineering Conf., Cairo, Egypt, (1995) pp. 151–161.
16. H. ARIK, S. KADİR and S. SARITAŞ, Tr. *Journal of Engineering and Environmental Sci.* **20** (1996) 233.
17. Y. SARIKAYA, N. BİÇER, C. BİÇER, H. CEYLAN and İ. BOZDOĞAN, Proceedings of the 3rd National Clay Symposium, Ankara, Turkey (1987).
18. P. D. RAMESH and K. J. RAO, *Mater. Res. Soc.* **9** (1994) 2330.
19. D. S. PERERA, *J. Mater. Sci.* **22** (1987) 2411.
20. Y. SUGAHARA, H. HIRAIWA, K. KURODA and C. KATO, *J. Mater. Sci.* **23** (1988) 3181.
21. K. J. D. MACKENZIE, R. H. MEINHOLD, G. V. WHITE, C. M. SHEPPARD and B. L. SHERRIFF, *J. Mater. Sci.* **29** (1994) 2611.
22. D. H. PECK, J. Y. KIM and S. W. CHOI, *Key Engin. Mater.* **89-91** (1994) 15.

Received 24 June
and accepted 21 August 1998